Fabrication of hard-shell microcapsules containing inorganic materials

Tamaru, Masato
Suzuki, Hiroshi
Hidema, Ruri
Komoda, Yoshiyuki
Suzuki, Kosuke

(Citation)
International Journal of Refrigeration,82:97-105

(Issue Date)
2017-10

(Resource Type)
journal article

(Version)
Accepted Manuscript

(URL)
https://hdl.handle.net/20.500.14094/90005592

Fabrication of Hard-Shell Microcapsules Containing Inorganic Materials

Masato TAMARU[1)], Hiroshi SUZUKI[1),2)*], Ruri HIDEMA[1),2)], Yoshiyuki KOMODA[1),2)] and Kosuke SUZUKI[1)]

[1)]Department of Chemical Science and Engineering, Kobe University,

[2)] Complex Fluid and Thermal Engineering Research Center, Kobe University,

1-1, Rokkodai-cho, Nada-ku, Kobe, Hyogo, 657-8501 Japan

*Corresponding Author, email:hero@kobe-u.ac.jp, Tel/Fax:+81-78-803-6490

Abstract

The fabrication method of silica hard shell microcapsules containing disodium hydrogen phosphate dodecahydrate ($Na_2HPO_4 \cdot 12H_2O$) has been developed. The effects of the mixing rates for the emulsification, of the volume ratios of solutions and of surfactant concentrations on the size of hollow microcapsules have been also studied. From the results, it was confirmed that silica hard shell microcapsules can contains $Na_2HPO_4 \cdot 12H_2O$ with the present method using hollow microcapsules. The present micro-encapsulated $Na_2HPO_4 \cdot 12H_2O$ was also found to cause the supercooling depression effect. As the fabricated microcapsules have no flammability, the present microcapsule was concluded to be a promising item not only for latent heat transportation media but also for the static thermal storage materials for architectural structures. From the studies on the fabrication parameters, it was concluded that the control of the surfactant concentration is effective for controlling the size of microcapsule.

Abbreviations

DSC, differential scanning calorimetry; HSMC, hard-shell microcapsule; PHPS, perhydropolysilazane; OP; oil phase; SEM, scanning electron microscope; WP; water phase

Keywords

Microcapsule, Phase Change Material, Inorganic Hydrate, Latent Heat

1. Introduction

1.1 Background

The thermal energy consumption for air-conditioning and hot water supply in residential and commercial areas in Japan increases to 2.0×10^{18} J per year (2.0 EJ y^{-1}) that is 50 to 60 % of total energy consumption of these areas. On the other hand, unused thermal energy exhausted from industries, power plants etc. is totally 2.5 EJ y^{-1} (Kasagi, *et al.*, 2013). Additionally, there exists other kind of unused thermal energy such as solar energy, geothermal energy, etc. Thus, the thermal energy consumption used in residential and commercial areas can be drastically reduced if those unused thermal energies can be utilized and be transported from heat sources as industries.

Recently, energy conversion technologies such as binary systems, which generate electric energy from the thermal energy has attracted many researchers. However, such an energy conversion system has very low conversion rate, which is less than 5%. Especially, it cannot utilize the thermal energy at less than 100^{o}C. This kind of low rank thermal energy has been wasted into rivers or sea. However, it has enough potential to use for air-conditioning and hot water supply used in residential and commercial areas. The efficiency of directly utilizing the unused thermal energy as thermal energy is much larger than that of energy conversion.

On the other hand, there exist time and space gaps between the demand and the supply in utilization of the unused thermal energy. This is called the thermal gap problem. In order to solve this problem, the thermal storage technology as static thermal storage systems and the thermal energy transportation technology as latent heat transportation systems should be candidates for the time gap and for the space gap, respectively.

1.2 Static Thermal Energy Storage

On the static thermal storage, some phase change materials have been already utilized, such as paraffin, inorganic materials and etc. Paraffin has an advantage in cost and it has no supercooling in its solidification. Thus, it is widely used as a phase change material for static thermal storages. However, it has high flammability. Then, it cannot be used for architectural structures. On the other hand, inorganic materials generally have no flammability and high stability, but generally show very large supercooling. Thus, there exist no suitable phase change materials used for the thermal storage in architectural structures.

1.3 Latent Heat Transportation

In order to solve the space gap between the demand and the supply of thermal energy, latent heat transportation systems have attracted in a field of the building air-conditionings and of district heating/cooling systems. Latent heat transportation systems containing fine phase change particles in water have three times high density of heat compared with that of water sensitive heat transportation systems. Then, the flow rate can be reduced and it causes to save the pumping power for transportation. Additionally, it has temperature sustainability in heat exchangers. Then, heat transfer characteristics can be improved.

Ice/water slurries have been studied as latent heat transportation media because it is cheapest among latent heat transportation systems. Fukusako *et al.* (2000) and Inaba *et al*. (2005) summarized the resent studies on ice/water slurries. However, the phase change temperature of ice/water slurries is too low for the normal air-conditioning. Then, a clathlate hydrate system such as tetrabutylammonium chloride hydrate (Fukushima *et al*., 1999, Darbouret *et al*., 2005, Ma *et al.*, 2012, Kumano *et al.*, 2012),

and trimethylolethane hydrate which have the phase change temperature about 10°C were investigated for cooling systems (Indartono *et al*., 2006, Suzuki *et al*., 2006, Suzuki *et al.*, 2009, Suzuki *et al.*, 2010b). Among them, tetrabutylammonium chloride hydrate slurries have been already utilized in actual systems (Fukushima *et al*., 1999).

On the other hand, very few materials for heating system have been studied, even though the high temperature heat about 50°C is required in residential and commercial area and its energy consumption is much larger than that of cooling system. Suzuki *et al*.(2010a, 2012, 2013) reported some inorganic hydrate systems are effectively for latent heat transportation systems. The reason why the high temperature latent heat transportation is not realized is that the particles in slurries grow at room temperature due to the phase change while the particles in low temperature latent heat transportation systems used for cooling systems disappear due to melting and that the inorganic hydrate particles easily adsorb onto the walls in heat exchangers. These causes a sever accident of pipe blocking at room temperature after the system is shut down. Toyoda *et al*. (2014a) reported the improvement of the adsorption characteristics of ammonium alum hydrates and Hidema *et al*.(2014a, 2014b) reported some additives can prevent the particle growth of ammonium alum hydrates. However, the particle growth depression technologies has not yet been completed. Thus, there exist no examples on high temperature transportation to be applied to an actual system.

1.4 Microcapsule

Some microcapsules containing phase change materials have been reported and applied to an actual latent heat transport system. The shell of those microcapsules is made of some resin and the microcapsules contain paraffin in its inside (Zhang *et al.*, 2004, Alvarado *et al*., 2007, Zhang *et al.*, 2010, Sari *et al.*, 2010, Tumirah *et al.*, 2014).

As the phase change materials are covered by shells, the particle does not grow in its size. Then, the microcapsules have an advantage compared with the slurries mentioned above. However, the resin shell cannot be used in high temperature and has disadvantages in mechanical strength and in chemical stability. The phase change material of paraffin has high flammability. Thus, it is difficult to use for high temperature latent heat transportation systems and for architectural structures.

Recently, silica hard shell microcapsules have attracted in the various use (Fujiwara *et al.*, 2004, Fujiwara *et al.*, 2010, Zhang and Hu, 2010)). Zhang *et al*. (2010) reported the fabrication method of silica hard shell microcapsules containing paraffin. Toyoda *et al.* (2014b) also reported that the fabrication of silica hard shell microcapsules containing trimethylolethane hydrates. Such a silica shell has advantages in mechanical strength, in chemical stability and it has low adsorption characteristics onto the metal walls. Additionally, it can be applied to the high temperature latent heat transportation because its melting point locates over 600^{o}C. Toyoda *et al.* (2014b) made the silica microcapsules from the porous hollow microcapsules. This technology indicates any materials with the phase change temperature of lower than 600^{o}C can be inserted into the microcapsules.

1.5 Purpose of the study

In this study, silica hard shell microcapsules (HSMCs) containing inorganic phase change materials have been fabricated as following the method reported by Toyoda *et al.* (2014b). Toyoda *et al.* (2014b) also reported that supercooling depression occurs in such a micro-encapsulated phase change material. Then, it is expected that the low supercooling inorganic phase change material can be realized with the present fabrication. As the whole microcapsule is made of inorganic materials, this

phase change materials have no flammability, and then can be applied to architectural structures as a static thermal storage system.

It is also important to control the size of microcapsules for latent heat transportation system. In this study, the method for controlling the size of microcapsules has been also investigated. The mixing rate and the mixing time for preparing emulsions, volume ratio of each solution, and the surfactant concentration used for emulsification were changed in some steps. From the results, the control method of the size of microcapsules will be also reported in this study.

2. Materials and Experimental details

2.1 Materials

In this study, disodium hydrogen phosphate dodecahydrates ($Na_2HPO_4 \cdot 12H_2O$) was adopted as a phase change materials, because it has high latent heat of 264 $kJ \cdot kg^{-1}$ (Telkes, 1980) and the phase change temperature of 30 wt% solution locates about 34^oC (Kenisarin and Mahvkamov, 2016). Thus, it has been expected to be suitable for heating media of air-conditioning systems. Suzuki *et al.*(2010a) reported the latent heat transportation system with this hydrate slurry. Disodium hydrogen phosphate has several hydration structures as reported by Telkes (1980), Magin *et al*. (1981) and Kenisarin and Mahvkamov (2016). In this study, the concentration of disodium hydrogen phosphate in water was set at 30 wt% as dodecahydrates of disodium hydrogen phosphate was obtained even in the cooling process.

2.2 Fabrication of Silica Microcapsules

A similar procedure as reported in the previous study (Toyoda *et al*., 2014b) was adopted in order to make silica hard shell microcapsules (HSMCs). At first, porous hollow silica microcapsules was made by following the method reported by Virtudazo *et al*. (2011) and Virtudazo *et al*. (2014) using a double-emulsion system based on interfacial reactions, as shown in Fig. 1. In the following, the basic recipe that is also shown in Fig. 1 is designated. Initially, 10.0 g of an aqueous sodium polymethacrylate (Na-PA; with the average molecular weight of 9,500) solution with the concentration of 30% in deionized water was mixed with 30.0 g of a sodium silicate (Na_2SiO_3) solution with the concentration of 30 wt% in deionized water. The deionized water was added to the solution as total amount became 36.0 ml. This water phase (the first phase solution) with polymer called as WP-1 was added to oil phase (the second phase solution as called OP) with 1.0 g of polyoxyethylene sorbitan monooleate (Tween80) and 0.50 g of sorbitan monooleate (Span80) as surfactants in 72.0 ml of *n*-hexane. The total weight ratio of surfactants in OP is 0.41wt%. The resulting two-phase solution (WP-1/OP) was emulsified by a homogenizer for 1 min at 8,300rpm. After this WP-1/O solution immediately poured into 250 ml of the third phase aqueous ammonium carbonate (NH_4HCO_3) solution (called WP-2) with the concentration of 2M. After 2 h stirring at 35^{o}C, the porous and hollow microcapsules were fabricated in the beaker. Fujiwara *et al.* (2004) reported this reaction process in the double-emulsion of WP-1/OP/WP-2. The porous and hollow microcapsules separated by a high speed centrifugation for 3 min at 4,000 rpm, washed one time by ethanol at first and then washed three times by water, dried at 100^{o}C for 12 h and sintered at 500^{o}C.

Figure 2 shows the encapsulating steps of the disodium hydrogen phosphate hydrates into the porous hollow microcapsule. The porous hollow microcapsules were soaked in a Na_2HPO_4 aqueous solution at 30 wt% in a test tube. The test tube was depressurized by a vacuum pump at 200 hPa for 1 h in order to remove the air from the inside of the porous hollow microcapsules. Subsequently, the silica microcapsules were filled with the Na_2HPO_4 solution. These microcapsules were separated from the solution by a suction filtration, and cooled and dried for 1 day in a refrigerator at 5^{o}C. In order to cover the holes of the silica porous microcapsules, a small amount of perhydropolysilazane (PHPS) solution was released in droplets on 0.3 g of the dried silica microcapsules under stirring as shown in Fig. 3. After stirred for 2 h, the silica microcapsules containing Na_2HPO_4 solution were dried for 1 day at room temperature. The microcapsules fabricated like this way were called as hard shell microcapsules (HSMCs).

2.3 Analysis of microcapsules characteristics

The fabricated porous and hollow microcapsules and enclosed microcapsules were observed by a scanning electron microscope (SEM). In this study, the SEM was used not only for observations of the morphology, but also for measurements of the shell thickness of microcapsules. In order to measure the shell thickness, microcapsules were cut by a microtome with cooling by electronic cooler at 0^{o}C and cut surface were observed by the SEM. The size of hollow microcapsules was measured by a laser diffraction/scattering particle size analyzer.

The melting/freezing points and the latent heat of the phase change materials in microcapsules were measured by a differential scanning calorimetry (DSC). From the

results of latent heat, weight and volume fractions of phase change materials in HSMCs was also calculated. The heating rates and cooling rates were fixed at 1 $K \cdot min^{-1}$ and -1 $K \cdot min^{-1}$. Na_2HPO_4 30wt% aqueous solution without encapsulation was also measured by the DSC. In order to confirm the repeatability, the latent heat measurements of the HSMCs containing Na_2HPO_4 30wt% aqueous solution were repeated in ten times.

2.4 Microcapsule size and shell thickness control

In order to find the method of the microcapsule size control, the effects of the volume ratio of WP-1/OP/WP-2, the mixing rate of homogenizer, and the surfactant concentration were investigated in this study. Table 1 tabulates the experimental conditions.

The recipe of Sample 1 in Table 1 is the original fabrication method proposed by Virtudazo *et al* (2011). The mixing rate in the cases from Samples 2 and 3 was changed from 5,000 to 2,500 rpm while the other conditions were fixed at the basic recipe. In the cases from Samples 4 and 5, the volume ratio of WP-1/OP/WP-2 was change as 1/1/7, 1/4/7. In the cases from Samples 6 and 7, the volume ratio of WP-1/OP/WP-2 was change as 1/2/3.5, 1/2/14. In the cases from Samples 8 to 10, the concentration of surfactants was changed from 0.13 to 0.83wt% while the surfactant ratio of polyoxyethylene sorbitan monooleate to sorbitan monooleate was kept at 2. The experiments were performed by the same procedure except these parameters.

The size of porous hollow microcapsules was also measured by a laser diffraction/scattering particle size analyzer. Moreover, the shell thickness of the

samples 1 and 8 to 10 are also investigated. Each sample is cut by a microtome, and observed by SEM.

3. Results and discussion

3.1 Microcapsules

Figures 4(a), (b) and (c) show SEM images of a hollow porous microcapsule, of a cut surface of a hollow porous microcapsule and of a coated microcapsule with the original recipe of Sample 1 reported by Virtudazo *et al* (2011).

As this Fig. 4(a) shows, it is confirmed that the micro-order capsules are formed and their surfaces have many nano-order-size holes (nano-holes). Figure 5 shows a size distribution of hollow porous microcapsules. As this figure shown, diameters of most microcapsules are over 10 μm, and the mode diameter is 24.8 μm. It is confirmed from Fig. 4(b) that the microcapsule has the hollow structure. A histogram of the shell thickness was made with one hundred samples of SEM images of such cut microcapsules as Fig. 6. From this figure, it is found that the mode shell thickness is 2.80 μm. From Fig. 4(c), it is found that the nano-holes of hollow porous microcapsules are closed by PHPS coating. The thickness of the shell of coated microcapsules are shown in Fig. 7. It was also measured with cut surface by SEM. The mode shell thickness is 3.10 μm. From this, it is found that the coated thickness is 0.3 μm and the diameter of coated microcapsules is 25.4 μm. Thus, the mean void fraction in the hollow microcapsule with the original recipe was determined as 43.2 vol%

3.2 Latent heat

The DSC curves of silica hard shell microcapsules containing 30 wt% aqueous solution of Na_2HPO_4 in HSMCs and 30wt% solution of Na_2HPO_4 without encapsulation are shown in Fig. 8. The solid curve in Fig. 8 indicates the results of the 1st run and the broken line designated ones of the 10th run for encapsulated cases. The chain line is the results of 30wt% solution of Na_2HPO_4 without encapsulation. The melting and freezing points were defined at the cross point of a base line and of a tangential line drawn from the minimum and maximum points of the DSC curve, respectively, as an example of the definition is shown in the case of the 1st melting in the figure.

At first, we discuss phase change temperatures of each sample. The melting point of phase change material in HSMCs locates at 32.6°C in the case of the 1st run, at 31.9°C in the case of the 10th run and one of 30 wt% solution without encapsulation is 33.9°C. Thus, it is confirmed the melting point of the present encapsulated materials agree with one of the solution without encapsulation and one by Kenisarin and Mahvkamov (2016). It is also found that the melting point in the case of 1st run is almost the same as one in the case of 10th run. Thus, it was confirmed that HSMCs contains $Na_2HPO_4 \cdot 12H_2O$ and that the present phase change in HSMCs is repeatable. The freezing point locates at 31.9°C in the case of the 1st run and at 29.2°C in the case of the 10th run. The supercooling degree of the solution in HSMCs is found to be very small as 0.7 K at the 1st run. The supercooling degree slightly increases with repeating, but it takes a still low value of 2.7 K even at the 10th run. On the other hand, the freezing point of the solution without encapsulation is 7.74°C. Thus, it is found the original solution of Na_2HPO_4 has a very large supercooling degree of 26.2 K. Toyoda *et al*. (2014b) reported trimethylolethane clathrate hydrates in HSMCs has a very small supercooling degree about 2 K. In general, inorganic hydrate materials show very

large supercooling. It is confirmed that the supercooling depression in HSMCs occurs even in the case of inorganic hydrate materials. The mechanism of such depression of supercooling has not been clarified. However, it is a promising feature to apply HSMCs not only to the latent heat transportation systems but also to the static thermal storage systems.

It is known that the amount of the latent heat of pure $Na_2HPO_4 \cdot 12H_2O$ is 264 $kJ \cdot kg^{-1}$ (Telkes, 1980). Then, the amount of the latent heat of Na_2HPO_4 30wt% aqueous solution has 198 $kJ \cdot kg^{-1}$. HSMCs containing Na_2HPO_4 30wt% solution has the latent heat of 52.5 $kJ \cdot kg^{-1}$ averaged for ten-time runs. From this, the weight fraction of $Na_2HPO_4 \cdot 12H_2O$ in HSMCs is calculated as 26.3 wt%. The density of Na_2HPO_4 30wt% solution measure by a gravimeter was 1,165 $kg \cdot m^{-3}$ at 45^{o}C and the density of silica is 2200 $kg \cdot m^{-3}$. Then, from this weight fraction obtained by the latent heat, the volume fraction of Na_2HPO_4 30wt% solution in HSMCs can be calculated as 40.2 vol%. As mentioned above, the void fraction in HSMCs is calculated from the microcapsule sizes as 43.2 vol%. The amount of the latent heat in HSMCs agrees well with the estimation obtained by the void fraction of HSMCs. Thus, it is confirmed that the HSMCs is almost fully occupied by Na_2HPO_4 30wt% solution.

3.3 Microcapsule size and shell thickness control

In order to investigate a method for controlling the size of silica microcapsules, the parameter study has been performed under the conditions tabulated in Table 1. The effects of parameters on the microcapsule size were evaluated by the measurements only for the porous hollow microcapsules in this study, because the final size of HSMCs significantly depends on the porous hollow microcapsules and the coating thickness was

very thin as described above. In the followings, the mode diameter of the porous hollow microcapsules measured by a laser diffraction / scattering particle size analyser was shown in Figs 9, 10 and 11(a). The mode shell thickness measured from the SEM photos was shown in Fig. 11(b)

3.3.1 Effects of the mixing rate

Figure 9 shows the effects of mixing rate with the homogenizer. The results of Samples 1 to 3 are plotted in the figure. From this figure, it is found that mixing rate does not affect the size of microcapsules under the present conditions. This is because the shear rate added to the emulsion in the present homogenizer is very high enough for forming fine emulsion.

3.3.2 Effect of the volume ratios

Figure 10 (a) and (b) show the effects of the volume ratio of OP to WP-1 and of the volume ratio of WP-2 to WP-1, respectively. In Fig. 10(a), the results of Sample 1, 4 and 5 are plotted and those of Sample 1, 6 and 7 are plotted in Fig. 10(b). The other parameters were fixed as the mixing rate of 8,200 rpm, the surfactant concentration of 0.41 wt% and the mixing time of 60 s.

From Fig. 10(a), it is found that the size of microcapsules takes a constant value in each volume ratio of OP to WP-1. Thus, the volume ratio of OP to WP-1 does not affect on the microcapsule size.

From Fig. 10(b), it is found that the size of microcapsules takes a slightly lower at a low volume ratio of WP-2 to WP-1. It slightly increases with the volume ratio and takes a constant value at a high volume ratio. However, the effect of the volume ratio of WP-2 to WP-1 is not so large on the microcapsule size under the present conditions.

3.3.3 Effect of surfactant concentration

Finally, the effect of surfactant concentration is shown in Fig. 11. The results of Sample 1 and 8 to 10 are plotted in the figure.

From Fig. 11(a), it is found the size of microcapsules decreases with the surfactant concentration. This is considered to occur corresponding to the size of emulsion formed in the mixing process by a homogenizer. Large amount of surfactants sufficiently covers the surface of WP-1 droplets and can stabilize the many emulsion droplets. Thus, the microcapsules become small. The decrease tendency with surfactant concentration is almost linear. From the results of the present parameter study, it is concluded that the surfactant concentration is the effective factor to control the size of microcapsules.

The mode shell thicknesses are plotted in Fig. 11(b). From these figure, it is found that the shell thickness of microcapsules increases with the surfactant concentration. From the diameters shown in Fig. 11(a) and the shell thicknesses in this figure, the void fractions in the porous hollow microcapsules can be calculated. Figure 12 shows the results of the void fraction calculation. From this, it is found that the void fraction decreases with the surfactant concentration. Thus, the void fraction can be realized by decrease of surfactant concentration. However, much lower surfactant concentration causes instability of emulsion formation. There exists the optimum condition for the void fraction control.

Conclusion

In order to develop the fabrication method of the silica hard shell microcapsules containing inorganic phase change materials, a method using porous hollow microcapsules was suggested in this study. The method for controlling the size of microcapsules was also discussed though a parameter study.

From the results, it was confirmed that silica hard shell microcapsules can contains the inorganic phase change material of $Na_2HPO_4 \cdot 12H_2O$ with the present method using porous hollow microcapsules. The fabricated microcapsules have no flammability, no toxicity and chemical stability. The present micro-encapsulated $Na_2HPO_4 \cdot 12H_2O$ was also found to cause the supercooling depression effect. Thus, the present microcapsules can be a promising material not only for the latent heat transportation systems but also for the static thermal storage systems, which could be applied to architectural structures.

The surfactant concentration was found effectively to affect the size of porous hollow microcapsules. The size of microcapsules decreased with the surfactant concentration linearly. The shell thickness also increased with the surfactant concentration. Thus, it was concluded that the surfactant concentration is the most important factor for controlling the size and the void fraction control.

Acknowledgement

This study was partially supported by NEDO (New Energy and Industrial Technology Development Organization) project: "Incubation Research on Innovative Technologies in the Thermal Energy Storage Materials/Research and Development Project for Innovative Thermal Management Materials and Technologies".

References

Alvarado J.L., Marsh C., Sohn C., Phetteplace G., Newell T., 2007, Thermal Performance of Microencapsulated Phase Change Material Slurry in Turbulent Flow under Constant Heat Flux, *Int. J. Heat Mass Trans.*, 50: 1938-1952.

Darbouret M., Cournil M., Herri J.-M., 2005, Rheological Study of TBAB Hydrate Slurries as Secondary Two-Phase Refrigerants, *Int. J. Refrig.*, 28: 663-671.

Fukusako S., Kozawa Y., Yamada M., Tanino, M., 2000, Fundamental Researches and Developments on Fine Crystalline Ice Slurries in Japan, *Trans. JSRAE*, 17: 413-437.

Fukushima S., Takao S., Ogoshi H., Ida H., Matsumoto S., Akiyama T., Otsubo T., 1999, Development of High-Density Cold Latent Heat with Clathrate Hydrate, *NKK Tech. Rep.* 166:65-70.

Hidema R., Suzuki H., Tano T., Komoda Y., 2014a. Flow and Heat Transfer Characteristics of Ammonium Alum Hydrate Slurries with Surfactants as Drag-Reducers with Poly Vinyl Alcohol as Stabilizers, *Int. Heat Transfer Conf. 15*, DOI: 10.1615/IHTC15.fcv.009469

Hidema R, Tano T, Suzuki H, Fujii M, Komoda Y, Toyoda T., 2014b, Phase Separation Characteristics of Ammonium Alum Hydrates with Poly Vinyl Alcohol, *J. Chem. Eng. Jpn*. 47(2): 169-174.

Inaba H., Inada T., Horibe A., Suzuki H., Usui H., 2005, Preventing Agglomeration and Growth of Ice Particles in Water with Suitable Additives, *Int. J. Refrigeration*, 28: 20-26.

Indartono Y. S., Usui H., Suzuki H., Komoda Y., Nakayama K., 2006, Hydrodynamics and Heat Transfer Characteristics of Drag-Reducing Trimethylolethane Solution and Suspension by Cationic Surfactant, *J. Chem. Eng. Japan*, 39: 6: 623-632.

Kasagi N., Shikazono N., Suzuki I., Sekine Y., Nakamura R., 2013, *Technology Survey on Advanced Utilization Medium to Low Temperature Heat*, *JST Research Rep*., Japan Science and Technology Agency, Tokyo.

Kenisarin, M. and Mahkamov, K., 2016, Salt Hydrates as Latent Heat Storage Materials: Thermophysical Properties and Costs, *Solar Energy Mater. Solar Cell*s, 145: pp.255-286.

Kumano H., Hirata T., Mitsuishi K., Ueno K., 2012, Experimental Study on Effect of Electric Field on Hydrate Nucleation in Supercooled Tetra-n-Butyl Ammonium Bromide Aqueous Solution," *Int. J. Refrig.*, 35: 1266-1274.

Magin, R.L., Mangum, B.W., Statler, J.A., Thornton, D.D., 1981, Transition Temperatures of the Hydrates of Na_2SO_4, Na_2HPO_4 and KF as Fixed Points in Biomedical Thermometry, *J. Res. Nat. Bureau Stand.*, 86: 2: 181-192.

Sari A., Alkan S., Bilgin C., 2014, Micro/Nano Encapsulation of Some Paraffin Eutectic Mixtures with Poly(Methyl Methacrylate) Shell: Preparation, Characterization and Latent Heat Thermal Energy Storage Properties, *Appl. Energ.,* 136: 217-227.

Suzuki H., Itotagawa T., Indartono Y.S., Usui H, Wada N., 2006, Rheological Characteristics of Trimethylolethane Hydrate Slurry Treated with Drag-Reducing Surfactants, *Rheol. Acta*. 46: 287–295.

Suzuki H., Kishimoto T., Komoda Y., Usui H., 2010a, Investigation of Thermal Properties of Na_2HPO_4 Hydrate Slurries for Evaluating Their Use as a Coolant in Absorption Chillers, *J. Chem. Eng. Japan*, 43: 34-39.

Suzuki H., Konaka T., Komoda,Y., Ishigami T., 2013, Flow and Heat Transfer Characteristics of Ammonium Alum Hydrate Slurries, *Int. J. Refrig.*, 36: 81-87.

Suzuki H., Konaka T., Komoda Y., Ishigami T., Fudaba, T, 2012, Flow and Heat Transfer Characteristics of Ammonium Alum Hydrate Slurry Treated with Surfactants, *J. Chem. Eng. Japan*, 45: 136-141.

Suzuki H., Tateishi S, Komoda Y, 2010b, Effect of Molar Ratio of Counter-ions to Cationic Surfactants on Drag Reducing Characteristics of Trimethylolethane Hydrate Slurries, *Int. J. Refrig.,* 33: 1632-1638.

Suzuki H., Wada N., Komoda Y., Usui, H., Ujiie H., 2009, Drag Reduction of Trimethylolethane Hydrate Slurries Treated with Surfactants, *Int. J. Refrig.*, 32: 931-937.

Telkes M., 1980, Thermal Energy Storage in Salt Hydrates, *Solar Energy Matt.*, 2: 381-393.

Toyoda T., Hidema R., Suzuki H., Komoda Y., 2014a, Crystal Growth and Viscosity Behaviors of Ammonium Alum Hydrate Solution with PVA in Shear Flow, *Nihon Reoroji Gakkaishi*, 42: 219-226.

Toyoda T., Narisada R., Suzuki H., Hidema R., Komoda Y., 2014b, Fabrication Process of Silica Hard-shell Microcapsule (HSMC) Containing Phase-change Materials, *Chem. Lett*., 43(6): 820-821.

Tumirah K., Hussein M.Z, Zulkarnain Z, Rafeadah R, 2014, Nano-Encapsulated Organic Phase Change Material Based on Copolymer Nanocomposites for Energy Storage, *Energy,* 66: 881-890.

Virtudazo R.V.R., Fuji M., Shirai T., 2011, Fabrication of Calcined Hierarchical Porous Hollow Silicate Micro-Size Spheres via Double Emulsion Process, *Mater. Lett.*, 65: 3112-3115.

Virtudazo R.V.R., Wu R.T, Zhao S, Koebel M.M, 2014, Facile Ambient Temperature Synthesis and Characterization of a Stable Nano-Sized Hollow Silica Particles Using Soluble-Poly(Methacrylic Acid) Sodium Salt Templating, *Mater. Lett.,* 126: 92-96.

Zhang A, Hu Q, 2010, Adsorption of Cesium and Some Typical Coexistent Elements Onto a Modified Macroporous Silica-Based Supramolecular Recognition Material, *Chem. Eng. J.*, 159: 58-66.

Zhang H., Wang X., Wu D., 2010, Silica Encapsulation of n-Octadecane via Sol-Gel Process: A Novel Microencapsulated Phase-Change Material with Enhanced Thermal Conductivity and Performance, *J. Colloid Interf. Sci.*, 343(1): 246-255.

Zhang X.X., Fan Y.F., Tao X.M., Yick K.L., 2004 Fabrication and properties of microcapsules and nanocapsules containing ***n***-octadecane, *Mater. Chem. Phys*., 88: 300-307.

Captions

Table 1 Experimental conditions for investigating the effects of parameters on the porous hollow microcapsule size
Fig. 1 Schematic view of the preparing particles process and original recipe
Fig. 2 Vacuum degassing apparatus
Fig. 3 Schematic view of coating process
Fig. 4 SEM images (a) of a porous hollow microcapsule and (b) of the cut surface of porous hollow microcapsule (c) of a coated microcapsule by use of the original recipe
Fig. 5 Microcapsule size distribution by use of the original recipe
Fig. 6 Shell thickness distribution of porous hollow microcapsules by use of the original recipe
Fig. 7 Shell thickness distribution of microcapsules coated by PHPS
Fig. 8 The DSC curves of Na_2HPO_4 30wt% solution in HSMCs and without encapsulation
Fig. 9 Effect of mixing rate on microcapsule size
Fig. 10 Effect of volume ratio on microcapsule size (a) Volume ratio of OP to WP-1 (b) Volume ratio of WP-2 to WP-1
Fig. 11 Effect of surfactant concentration (a) Microcapsule size (b) Shell thickness
Fig. 12 Effect of surfactant concentration on void fraction

Table 1 Experimental conditions for investigating the effects of parameters on the porous hollow microcapsule size

Sample No.	Volume ratio (WP-1/OP/WP-2)	Surfactant concentration [wt%]	Mixing rate [rpm]	Mixing time [sec]
1	1/2/7	0.41	8200	60
2	1/2/7	0.41	4000	60
3	1/2/7	0.41	2500	60
4	1/1/7	0.41	8200	60
5	1/4/7	0.41	8200	60
6	1/2/3.5	0.41	8200	60
7	1/2/14	0.41	8200	60
8	1/2/7	0.10	8200	60
9	1/2/7	0.21	8200	60
10	1/2/7	0.82	8200	60

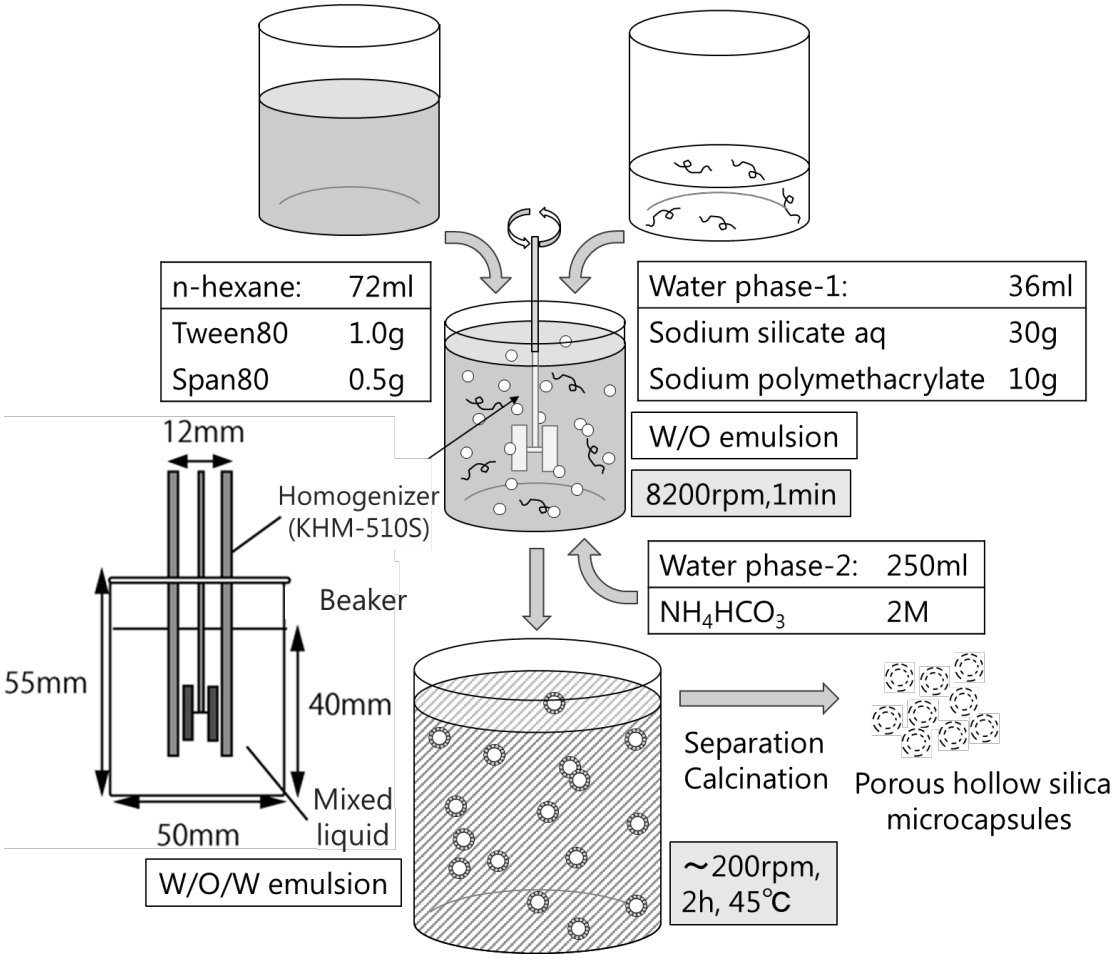

Fig. 1 Schematic view of the preparing particles process and original recipe

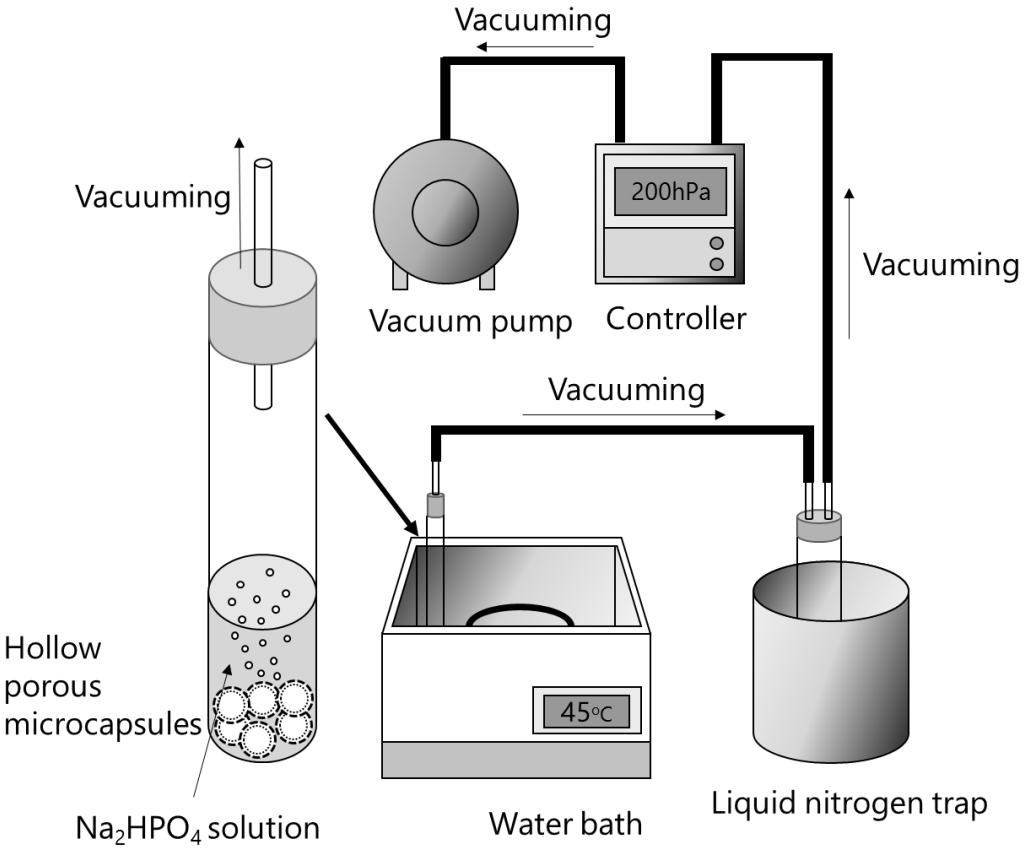

Fig. 2 Vacuum degassing apparatus

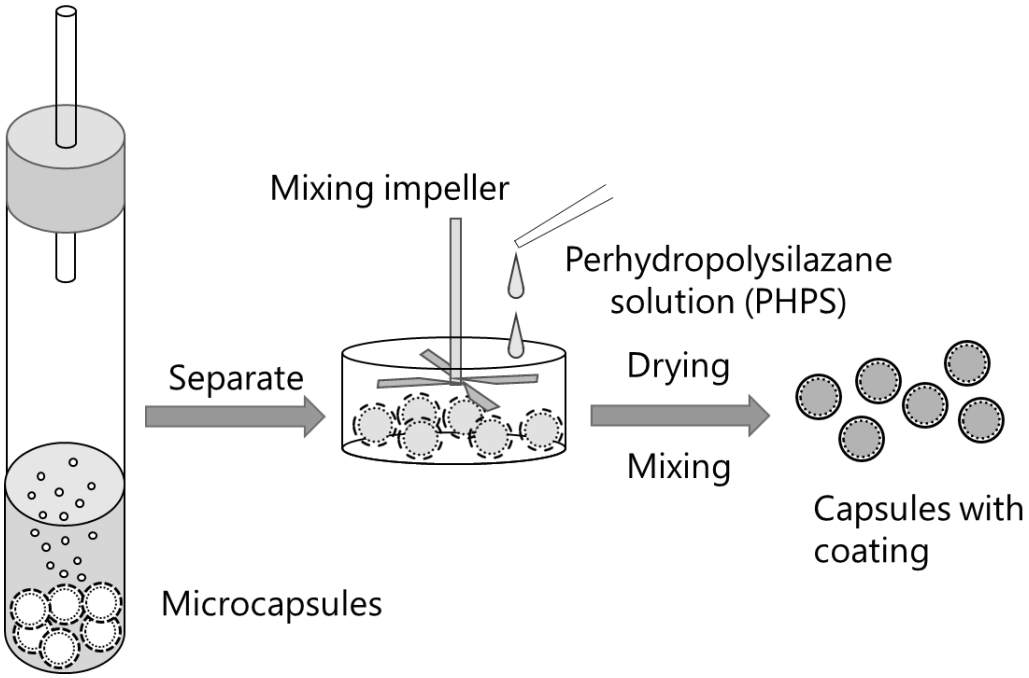

Fig. 3 Schematic view of coating process

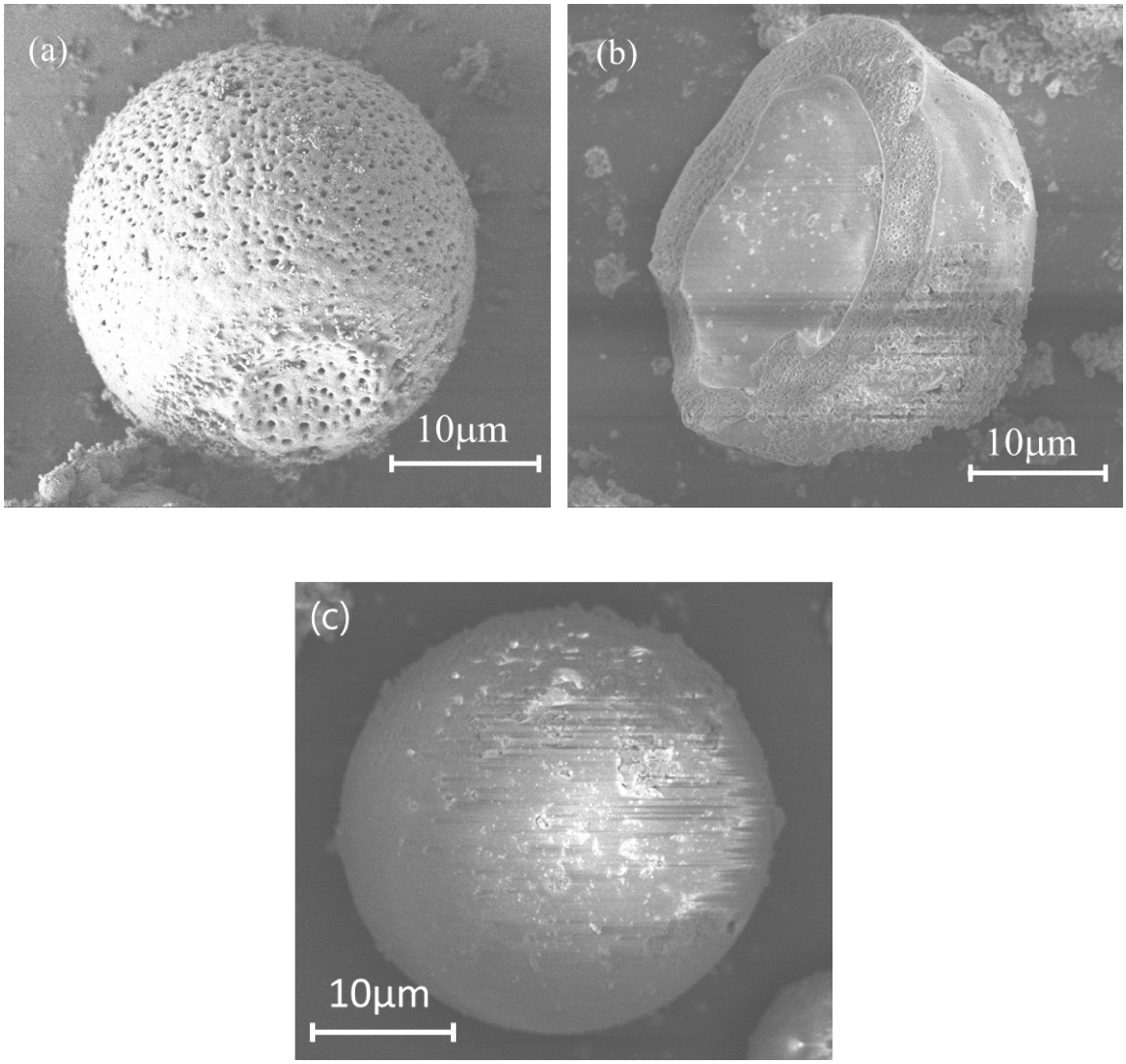

Fig. 4 SEM images (a) of a porous hollow microcapsule and (b) of the cut surface of porous hollow microcapsule (c) of a coated microcapsule by use of the original recipe

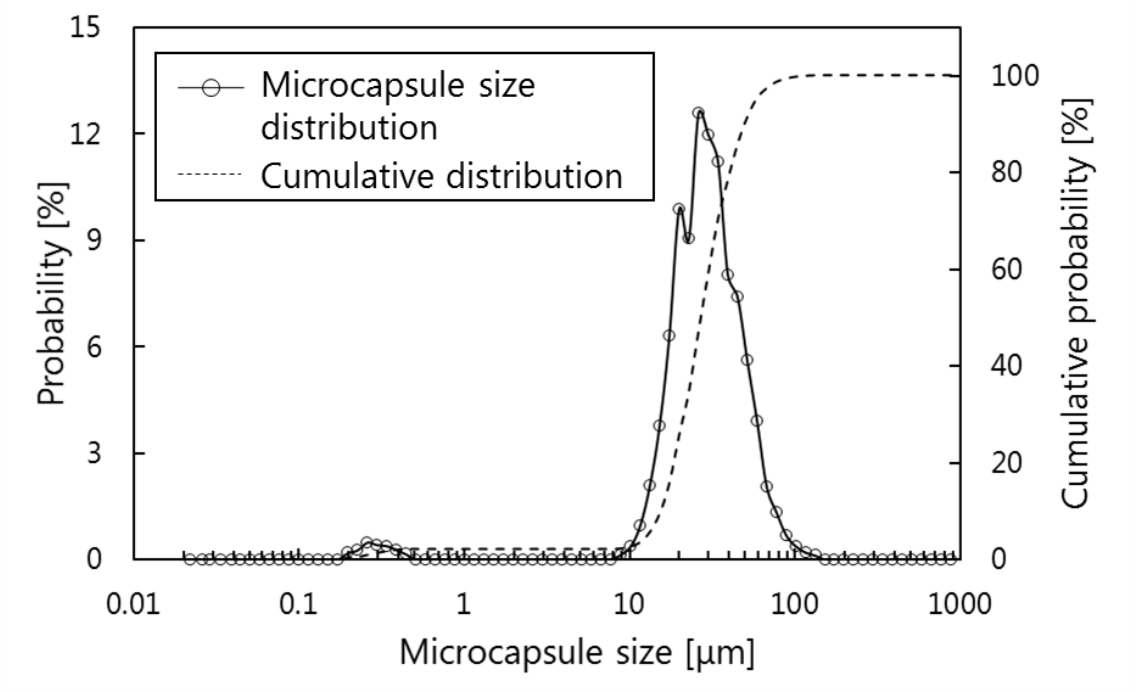

Fig. 5 Microcapsule size distribution by use of the original recipe

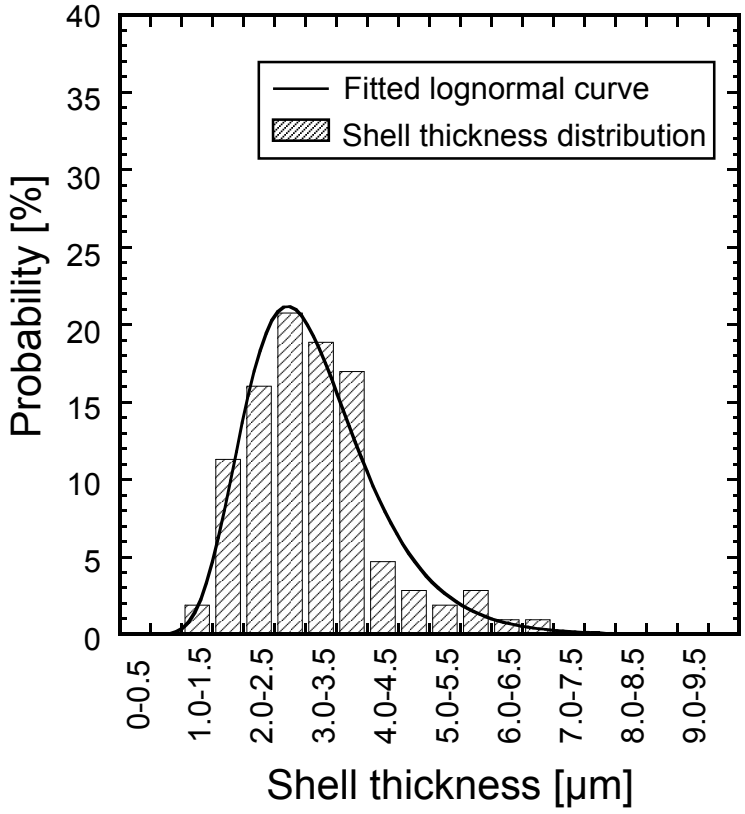

Fig. 6 Shell thickness distribution of porous hollow microcapsules by use of the original recipe

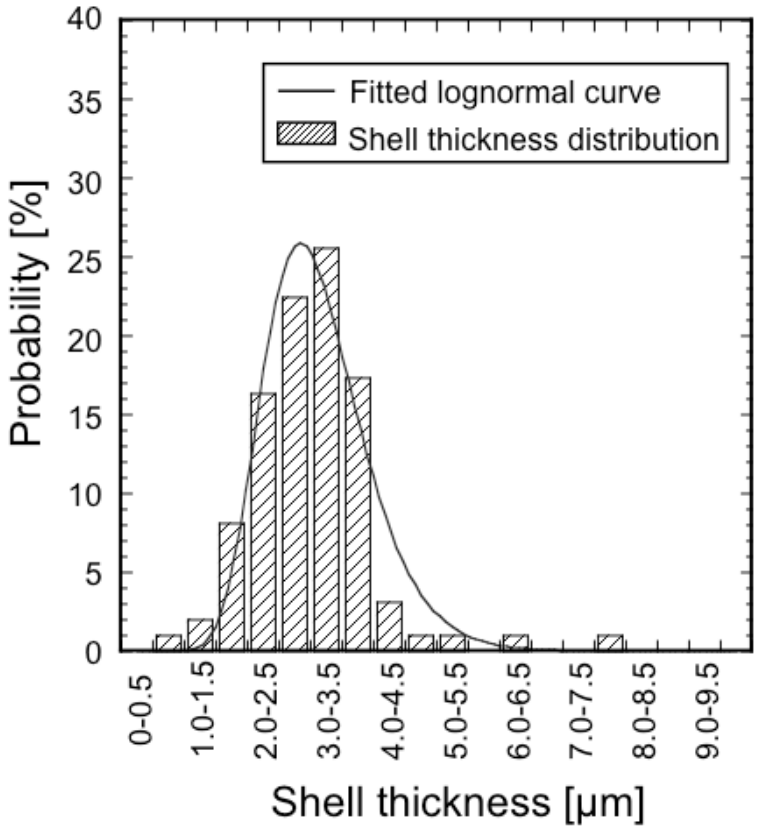

Fig. 7 Shell thickness distribution of microcapsules coated by PHPS

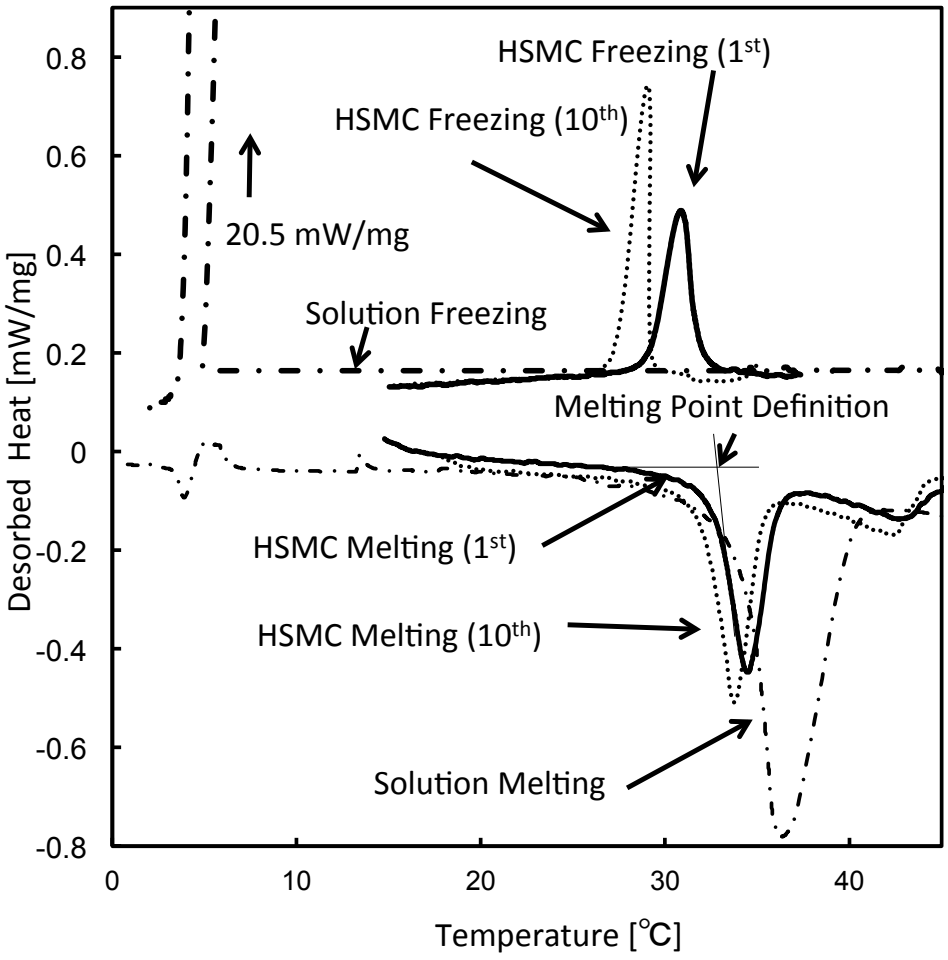

Fig. 8 The DSC curves of Na_2HPO_4 30wt% solution in HSMCs and without encapsulation

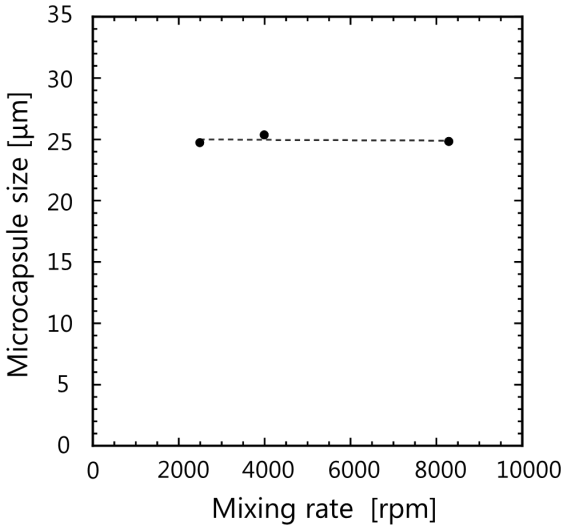

Fig. 9 Effect of mixing rate on microcapsule size

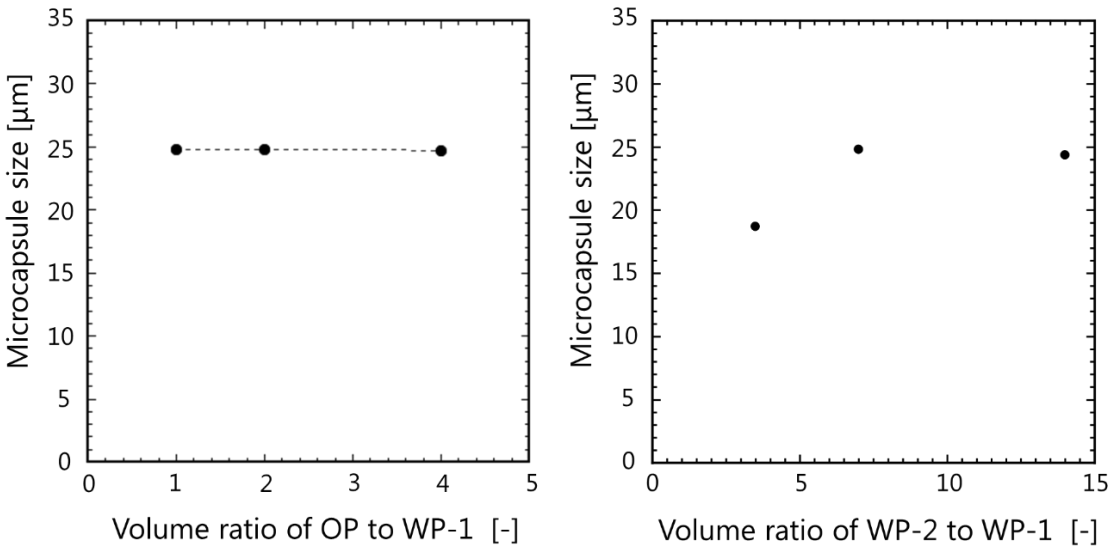

(a) Volume ratio of OP to WP-1 (b) Volume ratio of WP-2 to WP-1

Fig. 10 Effect of volume ratio on microcapsule size

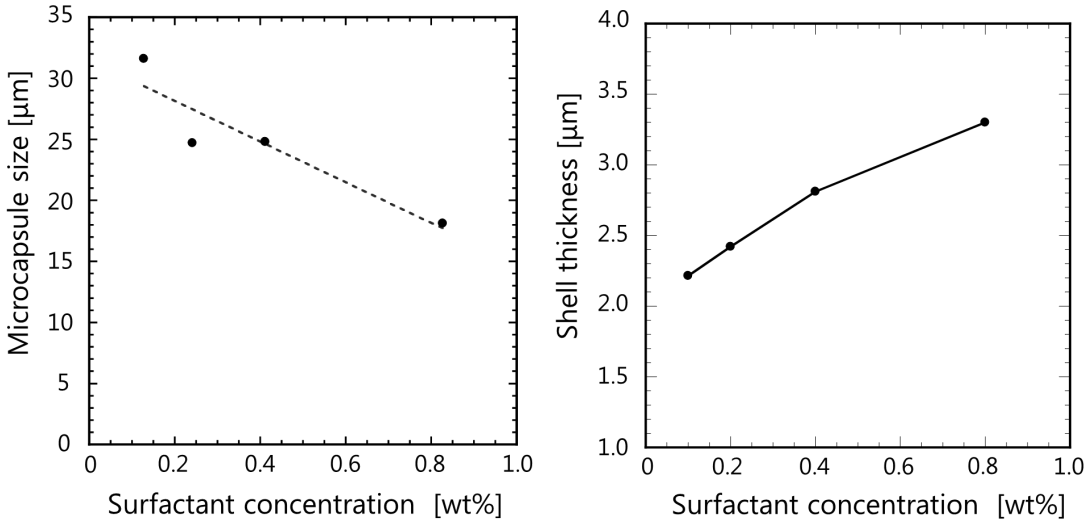

(a) Microcapsule size (b) Shell thickness

Fig. 11 Effect of surfactant concentration

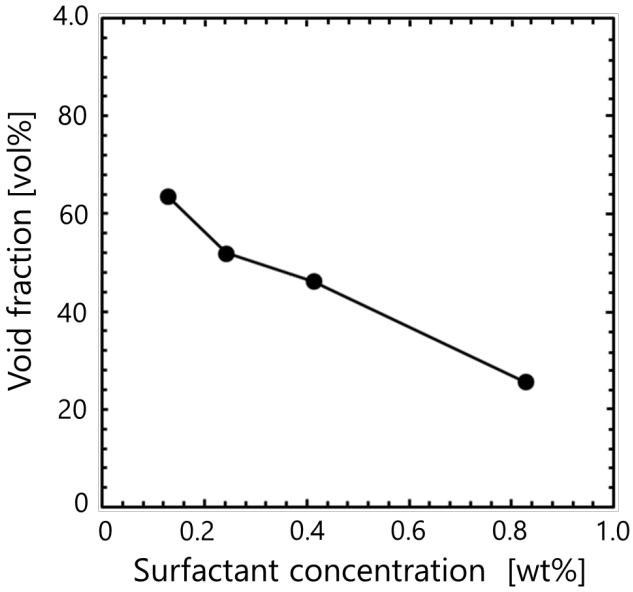

Fig. 12 Effect of surfactant concentration on void fraction